GEOLOGICAL SURVEY OF CANADA
OPEN FILE 7856

Targeted Geoscience Initiative 4: Canadian Nickel-Copper-Platinum Group Elements-Chromium Ore Systems — Fertility, Pathfinders, New and Revised Models

Magmatic Ni-Cu-PGE sulphide deposits at convergent margins

Graham T. Nixon[1], Matthew J. Manor[2], Sarah Jackson-Brown[2], James S. Scoates[2], and Doreen E. Ames[3]

[1]British Columbia Geological Survey, Victoria, British Columbia
[2]University of British Columbia, Vancouver, British Columbia
[3]Geological Survey of Canada, Ottawa, Ontario

2015

This publication is available for free download through GEOSCAN (http://geoscan.nrcan.gc.ca/)

Recommended citation

Nixon, G.T., Manor, M.J., Jackson-Brown, S., Scoates, J.S., and Ames, D.E., 2015. Magmatic Ni-Cu-PGE sulphide deposits at convergent margins, *In:* Targeted Geoscience Initiative 4: Canadian Nickel-Copper-Platinum Group Elements-Chromium Ore Systems — Fertility, Pathfinders, New and Revised Models, (ed.) D.E. Ames and M.G. Houlé; Geological Survey of Canada, Open File 7856, p. 17–34.

Publications in this series have not been edited; they are released as submitted by the author.

Contribution to the Geological Survey of Canada's Targeted Geoscience Initiative 4 (TGI-4) Program (2010–2015)

TABLE OF CONTENTS

Magmatic Ni-Cu-PGE sulphide deposits at convergent margins

Graham T. Nixon[1*], Matthew J. Manor[2], Sarah Jackson-Brown[2],
James S. Scoates[2], and Doreen E. Ames[3]

[1]British Columbia Ministry of Energy and Mines, British Columbia Geological Survey, PO Box 9333, Stn Prov Govt, Victoria, British Columbia V8W 9N3
[2]Pacific Centre for Isotopic and Geochemical Research, Department of Earth, Ocean and Atmospheric Sciences, University of British Columbia, 6339 Stores Road, Vancouver, British Columbia V6T 1Z4
[3]Geological Survey of Canada, 601 Booth Street, Ottawa, Ontario K1A 0E8
*Corresponding author's e-mail: graham.nixon@gov.bc.ca

ABSTRACT

Magmatic Ni-Cu-PGE sulphide deposits hosted by ultramafic-mafic intrusions in convergent-margin tectonic settings are an increasingly important resource worldwide, yet remain poorly understood and underexplored. A compilation of global mineralized intrusions in subduction-related settings underscores their economic potential and reveals mineralogical differences that may reflect parental magma composition and ore-forming processes. Our geochemical and isotopic investigations of two mineralized ultramafic intrusions in the Cordillera, the orthopyroxene-absent Turnagain Alaskan-type intrusion and the orthopyroxene-rich Giant Mascot intrusion, emphasize (1) the importance of wall-rock assimilation in promoting sulphide saturation and formation of an immiscible sulphide liquid; and (2) the ability of narrow conduit systems to channel influxes of new metal-laden magma and serve as traps for the collection of upgraded Ni-Cu-PGE sulphides. Processes fundamental to the production of economic Ni-sulphide deposits in the oxidized and hydrous primitive magmas generated at subduction zones are similar to those that have produced world-class magmatic nickel deposits in other tectonic settings.

INTRODUCTION

Investigations of orthomagmatic nickel-copper-platinum group element (Ni-Cu-PGE) mineralization in convergent-margin or supra-subduction-zone plate tectonic settings were carried out as part of the magmatic-hydrothermal nickel-copper-PGE ore system and convergent-margin Ni subprojects under the Targeted Geoscience Initiative 4 (TGI-4; Ames and Houlé, 2011; Ames et al., 2012). Our convergent-margin Ni-Cu-PGE study has a number of objectives: (1) examine the potential for economic Ni-sulphide deposits in an unconventional convergent-margin tectonic setting; (2) determine the principal factors that influence the genesis of magmatic Ni-Cu-PGE sulphide mineralization in the subduction-zone environment; and (3) evaluate exploration criteria for the discovery of economic mineralization in Canada and orogenic belts globally. To meet these objectives, we have (1) conducted a compilation of select global ultramafic-mafic intrusions that host Ni-sulphide deposits and prospects in convergent-margin settings; (2) investigated the ore-forming characteristics and mode of occurrence of Ni-Cu-PGE mineralization in two ultramafic intrusions in the Canadian Cordillera that have contrasting petrogenetic affiliations, including the Turnagain Alaskan-type intrusion, which characteristically lacks orthopyroxene, and the orthopyroxene-rich Giant Mascot intrusion; and (3) made a preliminary evaluation of factors that may influence the prospectivity of ultramafic-mafic intrusions at convergent margins for significant Ni-Cu-PGE mineralization. From our studies, which are summarized below, we contend that (1) the nature of ultramafic-mafic intrusions that host Ni-Cu-PGE mineralization at convergent margins is more diverse than generally realized; (2) the principal factors that promote magmatic sulphide mineralization in the relatively oxidizing environment of subduction zones are akin to those involved in the generation of major Ni-sulphide deposits in other tectonic environments; and (3) the potential for the discovery of economic deposits at convergent margins is currently underestimated.

CONVERGENT-MARGIN Ni-Cu-PGE DEPOSITS

Most of the world's major magmatic Ni-Cu-PGE deposits are hosted by ultramafic-mafic intrusions and volcanic rocks in various rift-related settings (summarized by Naldrett, 2010). Magmatic Ni-Cu-PGE sulphide deposits at convergent margins are becoming an increasingly important resource worldwide, yet are still

Nixon, G.T., Manor, M.J., Jackson-Brown, S., Scoates, J.S., and Ames, D.E., 2015. Magmatic Ni-Cu-PGE sulphide deposits at convergent margins, *In:* Targeted Geoscience Initiative 4: Canadian Nickel-Copper-Platinum Group Elements-Chromium Ore Systems — Fertility, Pathfinders, New and Revised Models, (ed.) D.E. Ames and M.G. Houlé; Geological Survey of Canada, Open File 7856, p. 17–34.

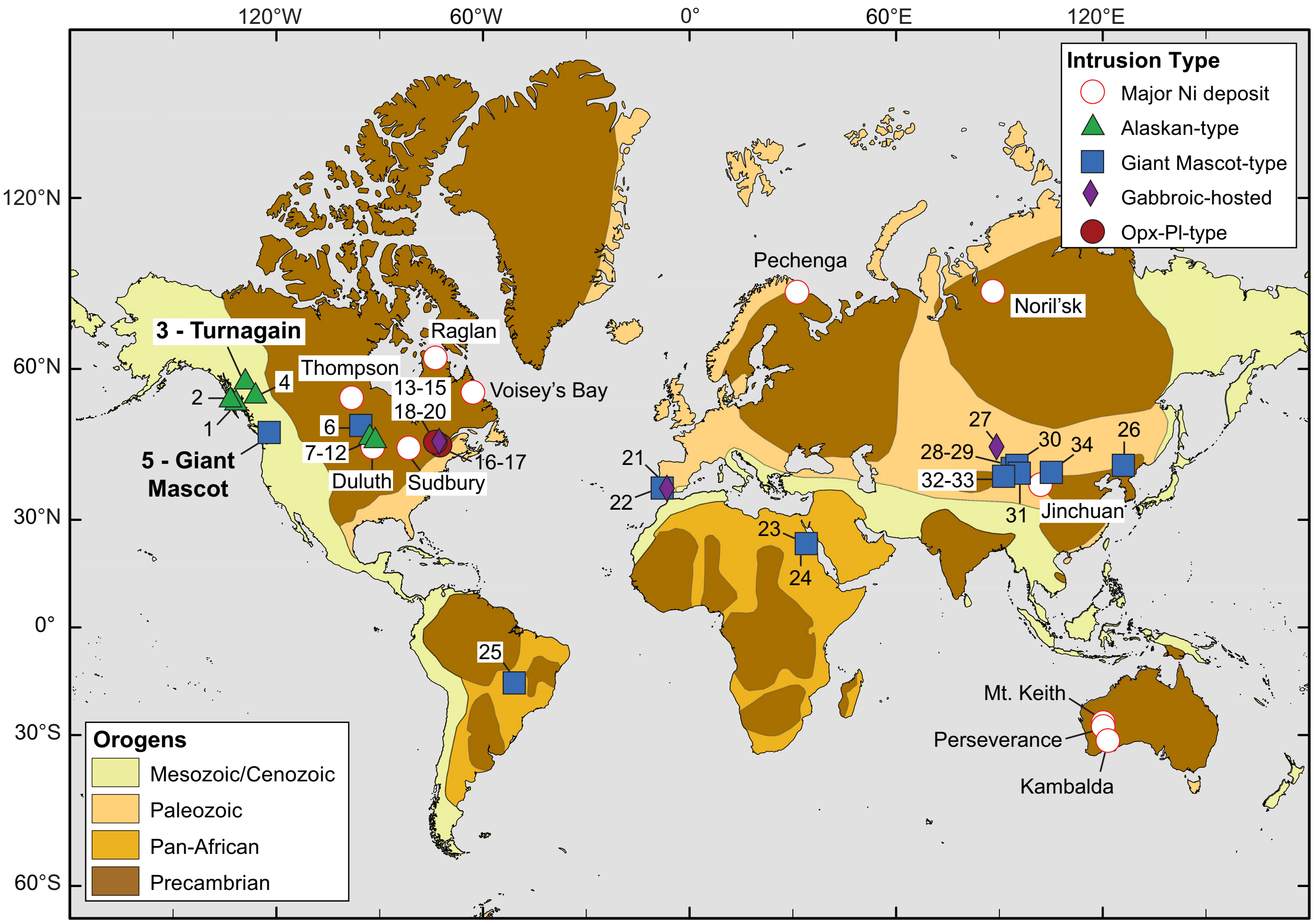

Figure 1. Global occurrences of selected orthomagmatic Ni-Cu±PGE deposits and prospects hosted by orthopyroxene-absent (Alaskan-type) and various orthopyroxene-rich ultramafic-mafic intrusions (Giant Mascot-type, gabbroic and orthopyroxene-plagioclase (Opx-Pl)-type) in convergent-margin plate tectonic settings, and world-class Ni-sulphide deposits/mining camps in other tectonic environments. Deposits listed in bold represent TGI-4 study locations. Numbered deposits/prospects correspond to those in Table 1 (generalized orogenic belts taken from Guillot et al., 2009; Mercator projection).

poorly understood and underexplored. Traditionally, subduction-zone settings have been regarded as unfavourable environments for nickel exploration due to the relative paucity of economically exploitable deposits. Consequently, mineral deposit models for magmatic Ni-sulphide mineralization at convergent margins have emerged only recently (e.g. Ural-Alaskan NC-7: Naldrett, 2010).

A compilation of selected global Ni-Cu±PGE deposits and prospects at convergent margins, which included factors such as age, host-rock characteristics, and other pertinent features, indicates that the occurrence of these deposits is more common and the number of similarities among them is greater than previously considered (Fig. 1, Table 1). All of the ultramafic-mafic intrusions that host Ni-sulphide mineralization that were compiled are in deformed and metamorphosed, arc-related accretionary terranes, and their ages range from Late Cretaceous (Giant Mascot, ca. 93 Ma) to Neoarchean (Gordon Lake and the Quetico intrusions, ca. 2.7 Ga; Table 1). All of these intrusions are reported to contain magmatic "hornblende" (typically tschermakite, pargasite, magnesiohornblende, magnesiohastingsite, and edenite), especially those with ultramafic suites. To aid in distinguishing different intrusion types, we have adopted a simple mineralogical classification (discussed below).

The intrusions are generally small (<4 km^2) and form composite or simple dykes, plugs, and sill-like bodies. They exhibit a well developed (rare) to crudely concentric, bilateral, or unilateral arrangement of rock units separated by sharp to gradational contacts, and have centimetre-scale (rare) to hectometre-scale (common) layering, or no discernible internal structure.

Intrusions considered to have been emplaced in supra-subduction regimes include Alaskan-type bodies in southeastern Alaska (Himmelberg and Loney, 1995), British Columbia (Nixon et al., 1997), and the Portneuf-Mauricie Domain intrusions in Quebec (Sappin et al., 2009, 2011). Although some intrusions bear the geochemical fingerprint of subduction-modified mantle source regions, such as the Permian intru-

Table 1. Global occurrences of selected magmatic Ni-Cu±PGE sulphide deposits and prospects in convergent-margin plate tectonic settings.

No.[1]	Type[2]	Deposit/ Prospect	Geotectonic setting[3]	Intrusion age (Ma)	Surface dimension	Internal structure	Intrusion lithologies[4]	Metamorphic grade[5]	Resource[6]	Grade (wt%) Ni	Cu
Southeast Alaska											
1	A	Duke Island (Marquis-Potato Patch-Raven)	Northern Cordillera/ Alexander terrane	Early Cretaceous (ca. 108–111)	23 km^2	composite/ layered/ crudelyzoned	dunite(±Cpx)/ wehrlite(±Hb)/ Ol clinopyroxenite(±Hb)/ Hb-Mt clinopyroxenite/ hornblendite(±Pl±Mt)	greenschist - amphibolite	prospect	<0.25	<2.8 (1g/t Pt+Pd)
2	A	Salt Chuck*		Silurian (ca. 430)	7.3 x 1.6 km	NIS	Bi-Pl-Mt clinopyroxenite(±Hb)/ Bi-Mt gabbro(±Hb)	greenschist	0.3 Mt		0.95 (2 g/t Pd)
British Columbia											
3	A	Turnagain (Horsetrail)	Northern Cordillera/ Yukon-Tanana terrane	Early Jurassic (ca. 190)	8.5 x 3 km	composite	dunite(±Cpx±Phl)/ wehrlite(±Phl)/ Ol clinopyroxenite/ Mt clinopyroxenite/ Hb clinopyroxenite(±Mt)/ hornblendite (±Pl±Bi)/ Hb diorite(±Bi)/ chromitite	lower greenschist	1841.8 Mt	0.21	(0.013 Co)
4	A	Polaris	Northern Cordillera/ Quesnellia/ Harper Ranch subterrane	Early Jurassic (ca. 186)	45 km^2	crudely zoned (asymmetric)	dunite(±Cpx±Phl)/ wehrlite(±Phl)/ clinopyroxenite (±Phl)/ Ol clinopyroxenite (±Phl)/ Hb/ hornblendite(±Pl±Bi)/ Hb clinopyroxenite(±Pl±Mt±Bi)/ gabbro-diorite(±Bi±Mt)	lower greenschist	prospect	0.25	1.2 (<1.3 g/t Pt; <1.8 g/t Pd)
5	GM	Giant Mascot*	Northern Cordillera/ Coast Plutonic Complex	Late Cretaceous (ca. 93)	3 x 1.3 km	composite/ zoned	dunite(±Opx±Hb±Cpx)/Hb harzburgite/ Hb lherzolite (rare)/ Hb orthopyroxenite(±Ol)/ Ol-Hb websterite (±Pl)/ Hb websterite(±Pl)/ hornblendite(±Pl±Cpx)/ Hb gabbro	amphibolite	4.2 Mt	0.77	0.34
Ontario											
6	GM?	Gordon Lake*	Superior/ English River subprovince	Neoarchean (ca. 2.7 Ga)	180 x 45 m	possible weak zoning	Hb harzburgite/ Hb lherzolite/ Ol-Px hornblendite/ rare Ol-Hb orthopyroxenite & Hb wehrlite	upper amphibolite - lower granulite	1.5 Mt	0.92	0.47 (0.9 g/t Pt+Pd)
7	A	Samuels Lake	Superior/ Quetico subprovince	Neoarchean (ca. 2.69 Ga)	600 x 300 m	zoned	Mt-Hb-Pl clinopyroxenite(±Bi)/ wehrlite(±Hb±Bi)/ Bi-Pl hornblendite/ Hb gabbro/ monzodiorite-diorite	upper greenschist - lower amphibolite	prospect	0.15–1.0	0.2–1.0 (<1.8 g/t Pd+Pt)
8	A	Plateau Lake			650 x 100 m	weakly zoned	Hb clinopyroxenite(±Bi±Pl)/ hornblendite(±Bi±Pl)	low-mid amphibolite	prospect	<0.73	<4.4 (<1.7 g/t Pd+Pt)
9	A	Kawene			500 x 70–130 m	crudely zoned	Hb wehrlite(±Bi)/Hb clinopyroxenite(±Ol)/ Cpx hornblendite(±Bi)/hornblendite(±Pl±Bi±Cpx)/ Hb gabbro(±Bi±Kf±Qz)	upper greenschist - lower amphibolite	prospect	<0.47	<1.1 (<5.9 g/t PGE)
10	A	Abiwin			200 x 40 m	NIS	hornblendite(±Pl±Bi)/ Hb gabbro(±Bi±Kf±Qz)	mid-amphibolite	prospect	<0.24	<2.1 (<1.4 g/t Pd+Pt)
11	A	Mudd Lake			800 x 10–100 m	NIS	hornblendite(±Pl±Cpx±Bi)/Cpx hornblendite(±Bi)/ Hb gabbro(±Bi±Kf±Qz)/diorite(±Bi±Kf±Qz)	upper greenschist - lower amphibolite	prospect	<0.1	<5.1 (<3.9 g/t Pd+Pt)
12	A	Chief Peter Lake			760 x 460 m	zoned	Hb wehrlite(±Bi)/hornblendite(±Bi±Pl)	greenscist - amphibolite	prospect	<0.24	<0.81 (<2.5 g/t Pd+Pt)
Québec[6]											
13	Opx-Pl	Lac Matte	Grenville/Portneuf-Mauricie Domain	Mesoproterozoic (ca. 1.4 Ga)	1.1 x 0.9 km	NIS	websterite-orthopyroxenite(±Ol±Pl)/norite/ gabbronorite/rare Pl harzburgite & lherzolite	amphibolite	prospect		
14	Opx-Pl	Lac Kennedy			1 x 0.5 km	layered	harzburgite/Pl websterite(±Ol)/gabbronorite/norite	amphibolite	prospect		
15	Opx-Pl	Lac Édouard*			300 m wide	layered	harzburgite/websterite-orthopyroxenite(±Ol±Pl)/ gabbronorite	amphibolite	0.082 Mt	1.5	0.5
16	G	Boivin			160 x 70 m	NIS	Pl-websterite/gabbronorite	amphibolite	prospect		
17	G	Rochette West			150 x 150 m	NIS	websterite(±Pl)/gabbronorite/norite	amphibolite	prospect		
18	Opx-Pl	Lac à la Vase (Rousseau)			3 x 0.8–1.8 km	zoned	lherzolite-wehrlite-harzburgite(±Pl)/websterite-orthopyroxenite(±Pl)/gabbronorite/norite/hornblendite	amphibolite	prospect		
19	Opx-Pl	Lac Nadeau			1.04 x 0.45+ km	zoned	lherzolite-harzburgite(±Pl)/websterite(±Ol±Pl)/Pl-orthopyroxenite/gabbronorite/norite/Qz-diorite	amphibolite	prospect		
20	Opx-Pl	Réservoir Blanc			unknown	NIS	norite/gabbronorite/anorthosite/gabbro/orthopyroxenite	amphibolite	prospect		

Table 1 continued.

No.[1]	Type[2]	Deposit/ Prospect	Geotectonic setting[3]	Intrusion age (Ma)	Surface dimension	Internal structure	Intrusion lithologies[4]	Metamorphic grade[5]	Resource[6]	Grade (wt%) Ni	Cu
Spain											
21	G	Aguablanca	Variscan/Santa Olalla Igneous Complex	Carboniferous (ca. 341)	<10 km^2	layered/ breccia pipe	Hb gabbronorite/norite/gabbro/anothosite/rare Hb dunite, rare Hb harzburgite, rare Hb websterite (±Ol±Pl)	amphibolite and greenschist	15.7 Mt	0.66	0.46 (0.47 g/t PGE)
22	GM	Tejadillas	Variscan/Cortegana Igneous Complex	Carboniferous (ca. 336)	1.4 x 0.7 km	zoned	Hb harzburgite(±Cpx±Phl)/gabbronorite(±Ol)/ norite-gabbro(±Hb±Phl)/Qz diorite	amphibolite	prospect	0.16	0.08
Egypt											
23	GM	Gabbro Akarem	Pan-African/Nubian shield	Neoproterozoic (ca. 973)	West: 3 x 0.5 km; East: 7 x 2 km	zoned	Cpx-Hb-Opx dunite/lherzolite(±Hb±Pl)/Pl websterite(±Ol±Hb)/hornblendite(±Ol±Pl)	'unmetamorphosed'	0.7 Mt	0.95 (Ni+	
24	GM	Genina Gharbia		Neoproterozoic (ca. 963)	9 x 3 km	zoned	Hb harzburgite(±Pl±Cpx)/Hb lherzolite(±Pl)/ Hb pyroxenite(±Ol±Phl)/Hb norite/Opx-Hb gabbro	'unmetamorphosed' (greenschist?)	prospect		
Brazil											
25	GM	Americano do Brasil*	Braziliano/Brazilia Belt/ Goiás Magmatic Arc	Neoproterozoic (ca. 626)	12 x 3 km	layered	S1: Pl-Hb websterite/gabbronorite; S2: dunite/ wehrlite/ lherzolite; G2: lherzolite/websterite	amphibolite-granulite	3.1 Mt	1.12	1.02
China											
26	GM	Hongqiling No.7*	CAOB/Xing'an-Mongolianterrane/ Hulan Group (early Paleozoic)	Late Triassic (ca. 216)	~130 m^2	NIS (dyke-like)	orthopyroxenite(±Phl±Pl±Hb)/harzburgite/norite	amphibolite (Early-Middle Triassic metamorphism)	0.2 Mt Ni 0.04 Mt Cu	2.31	0.63
27	G	Kalatongke* (Y1, Y2, Y3)	CAOB/Junggar Orogen/ Puerjin-Ertai terrane/ Nanmingshui Fm (Lower Carboniferous)	Permian (ca. 287)	<400 m x 150 m (5.2 x 0.5 km concealed)	composite/ layered (funnel-shaped/ tabular)	Bi-Hb-Ol norite/Bi-Hb norite/troctolite/ Qz-Bi-Hb diorite	greenschist; 20 m contact metamorphic aureole	Y1: 18 Mt Y2: 10 Mt Y3: 5 Mt	0.88 0.6 0.6	1.4 1.1 1.1
28	GM	Huangshandong* (Huangshan East)	CAOB/North Tianshan terrane/Gandu Group (mid-Carboniferous)	Permian (ca. 274)	3.5 x 1.2 km ~2.8 km^2	composite/ layered	Bi-Pl-Hb lherzolite/ Ol websterite(±Pl±Phl)/ gabbro/ Ol gabbro/ Hb gabbro/ troctolite/ gabbronorite(±Ol±Hb)/ Hb diorite(±Qz±Bi)	greenschist; weak contact metamorphic aureole <100m wide	>50 Mt 135 Mt	0.52 0.30	0.27 0.16
29	GM	Huangshanxi* (Huangshan)	CAOB/North Tianshan terrane/Gandu Group (mid-Carboniferous)	Permian (ca. 284)	3.8 x 0.8 km	composite/ layered	I. Hb lherzolite(±Pl)/gabbronorite; II. Hb-Bi gabbro(±Ol±Opx) III.Hb lherzolite(±Phl)/ Hb-Olwebsterite/ Ol orthopyroxenite(±Cpx±Hb)/ websterite	greenschist; weak contact metamorphic aureole <100m wide	80 Mt	0.54	0.3
30	GM	Hulu*	CAOB/North Tianshan terrane/Wotongwozi Fm (Lower Carboniferous)	Permian (ca. 282)	1.9 x 0.7 km	layered/ zoned (?folded sill)	Bi-Pl-Hb lherzolite-harzburgite; Hb-Pl pyroxenite/ Pl-Hb-Ol pyroxenite; Bi-Hb gabbro-diorite	amphibolite	80,200 t Ni 39600 t Cu	0.23-0.61	0.10–0.49
31	GM	Heishan	CAOB/Beishan terrane/Hulan Fm	late Devonian (ca. 366)	800 x 470 m	weakly zoned (dyke-like)	harzburgite(±Bi±Hb±Pl)/lherzolite	amphibolite?	35 Mt	0.6	0.3
32	GM	Poyi	CAOB/Beishan terrane/Pobei intrusion	Permian (ca. 271–284)	3 x 1 km	layered (pipe-like)	dunite/lherzolite(±Hb±Phl±Pl)/Ol websterite	upper greenschist?	1.3 Mt Ni 0.22 Mt Cu	0.5	
33	GM?	Poshi	CAOB/Beishan terrane/Pobei intrusion	Permian (ca. 271–284)	2 x 1.6	zoned	websterite(±Pl±Hb)/peridotite	upper greenschist?	14.7 Mt	0.3-0.6	
34	GM	Erbutu*	CAOB/Ondur Sum terrane/ Baoyintu Group (Meso-proterozoic)	Permian (ca. 294)	200 m x 170 m	layered	Ol orthopyroxenite(±Cpx±Hb±Phl)/ orthopyroxenite	amphibolite	1 Mt	0.3-2.0	

[1]Location shown in Fig. 1 [2] Intrusion type: A = Alaskan-type (orthopyroxene-free); GM = Giant Mascot-type (orthopyroxene-rich); G = gabbroic-hosted mineralization; Opx-Pl = orthopyroxene-plagioclase-hosted mineralization [3]CAOB = Central Asian Orogenic Belt; [4] Mineral abbreviations: Ol = olivine; Opx = orthopyroxene; Cpx = clinopyroxene; Hb = hornblende (magmatic amphibole); Phl = phlogopite; Bi = biotite; Pl = plagioclase; Kf = potassium feldspar; Qz = quartz [5] Metamorphic grade of host rocks to intrusion [6] Ore tonnage or contained metal tonnage where Ni and Cu indicated separately; Mt = million metric tonnes; t = metric tonnes [7] The Portneuf-Mauricie mafic-ultramafic intrusive suites are distinguished by early crystallizing plagioclase and minor amounts of late magmatic hornblende (Sappin et al., 2009) * Active or past-producing mine

References: 1) Irvine, 1974; Saleeby, 1992; Ripley et al., 2005; 2) Holt et al., 1948; Loney and Himmelberg, 1992; 3) Clark, 1975, 1980; Scheel, 2007; Nixon et al., 2012; Mudd and Jowitt, 2014; 4) Nixon et al., 1997; Simard et al., 2003; Mowat, 2013; 5) Aho, 1954, 1956; Manor, 2014; Manor et al., 2015a; 6) Scoates, 1972; Parker, 1998; 7) Pettigrew et al., 2000; Pettigrew and Hattori, 2006; 8-12) MacTavish, 1999; 13-14, 16-20) Sappin et al., 2009, 2011, 2012; 15) Mudd and Jowitt, 2014; Sappin et al., 2009, 2011, 2012; 21) Tornos et al., 2001, 2006; Piña et al., 2006, 2008, 2010; Romeo et al., 2006; 22) Piña et al., 2012; 23) Helmy and Mogessie, 2001; Helmy and Mallahawi, 2003; Helmy et al., 2005; 24) Helmy et al., 2014; Helmy, 2004; 25) Mota-e-Silva et al., 2011; Nilson, 1981; 26) Wu et al., 2004; Lu et al., 2011; Wei et al., 2013; 27) Li et al., 2012; Gao et al., 2012; Zhang et al., 2009: Han et al., 2004; 28) Gao et al., 2013; Mao et al., 2014a; Han et al., 2004; Zhang et al., 2011; Branquet et al., 2012; 29) Zhang et al., 2011; Mao et al., 2014b; Branquet et al., 2012; 30) Han et al., 2013; 31) Xie et al., 2012, 2014; 32) Xia et al., 2013; Qin et al., 2011; 33) Mao et al., 2008; Qin et al., 2011; 34) Peng et al., 2013.

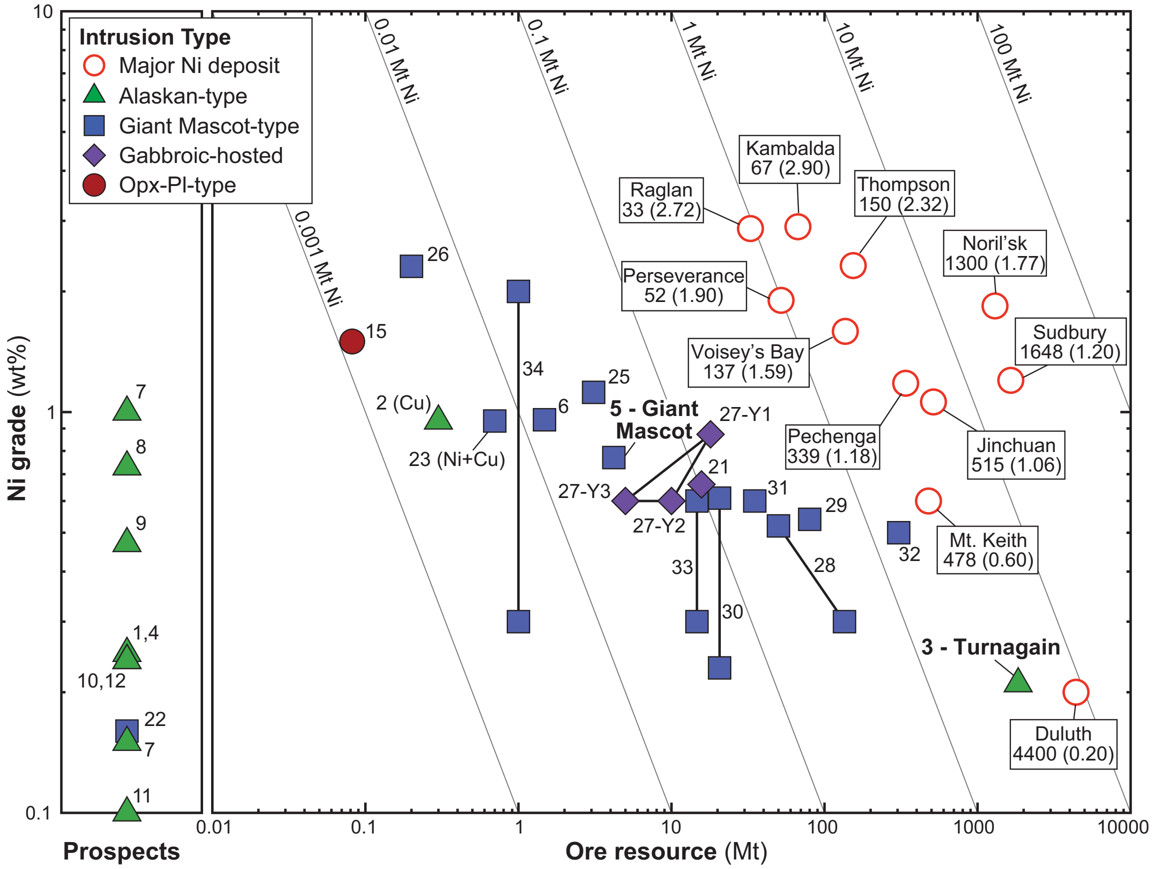

Figure 2. Ni grade in weight percent (wt%) versus ore tonnage in million metric tonnes (Mt) for the convergent-margin Ni-Cu±PGE deposits/prospects listed in Table 1 compared to world-class Ni-sulphide deposits (modified from Naldrett, 2010). Labels for major deposits denote tonnage (Mt) and wt% Ni grade (in brackets); numbered deposits and symbols correspond to those in Table 1 and Figure 1, respectively; diagonal lines represent contained Ni metal (note logarithmic scale).

sions in the Central Asian Orogenic Belt, they are regarded by some authors as "post-orogenic" (i.e. syn- or post-collisional) and are thought to be related to decompression melting of upwelling mantle asthenosphere that has been contaminated by a subduction component (Li et al., 2012; Sun et al., 2013a; Xia et al., 2013). Others consider these intrusions the result of a short-lived extensional event within the orogen generated by mantle plume activity (Zhang et al., 2010; Su et al., 2013). In the case of the Early Carboniferous (ca. 341 Ma) Aguablanca Ni-Cu-PGE deposit, which is Europe's only nickel mine, and the nearby Tejadillas prospect (ca. 336 Ma) in Spain, geochronological and geochemical data support the concept of an Andean-style convergent margin with a transpressional magmatic arc, whereas geophysical evidence has been used to invoke a mantle plume origin for the mineralized intrusions (Casquet et al., 2001; Tornos et al., 2001; Piña et al., 2006, 2010, 2012).

A plot of grade versus tonnage (Fig. 2) shows that significant Ni metal resources are contained in deposits formed in convergent-margin settings. Low-grade Ni-sulphide mineralization in the Turnagain Alaskan-type intrusion ranks among the top ten largest deposits in the world in terms of contained Ni metal, constituting a total resource of ~1842 Mt of ore with an average grade of 0.21 wt% Ni and 0.013 wt% Co (Mudd and Jowitt, 2014). Some of the largest Ni-Cu±PGE deposits being mined in China today are found in the accreted island arc terranes of the Central Asian Orogenic Belt, examples of which include the Kalatongke mine with ores grading ~0.6–0.9 wt% Ni and 1.1–1.4 wt% Cu; the 135 Mt Huangshandong deposit with a grade of 0.30 wt% Ni and 0.16 wt% Cu; and neighbouring Huangshanxi ores at 80 Mt with an average grade of 0.54 wt% Ni and 0.30 wt% Cu (Table 1). The total Ni metal resource for magmatic Ni-Cu sulphide deposits in the Huangshandong-Huangshanxi district alone approximates one million metric tonnes (Mao et al., 2008).

CLASSIFICATION: BACK TO THE FUTURE

Alaskan-type (Ural-Alaskan or concentrically zoned) intrusions in convergent-margin settings are well documented (e.g. Himmelberg and Loney, 1995; Nixon et al., 1997; Johan, 2002). The classic petrological studies of Taylor and Noble (1960), Noble and Taylor (1960), Taylor (1967), and Irvine (1974) were influenced by a concentric zonation of rock types in the larger bodies. They defined Alaskan-type intrusions as a distinctive suite of ultramafic(±gabbroic) rocks characterized by peridotite (dunite-wehrlite) in the core, passing outward into olivine clinopyroxenite, clinopyroxenite and hornblendite ± gabbro at the margin. The principal minerals forming the ultramafic rocks are olivine (+minor chromite) and clinopyroxene with magnetite and hornblende occurring in clinopyroxenite and hornblendite; orthopyroxene is typically absent and plagioclase is extremely rare. Cumulus textures are common and provide ample evidence for differentiation by crystal fractionation and mineral concentration processes. In general, Alaskan-type intrusions are considered to occur in sulphide-poor magmatic environments and are known primarily for their dunite-hosted, chromitite-PGE mineralization that provides most of the world's important platinum placer deposits (e.g. Tulameen, British Columbia, Nixon et al., 1990; Johan, 2002; Weiser, 2002).

Modern "petrotectonic" classification schemes for Ni-sulphide deposits tend to focus on the nature of parental magmas associated with rocks that host the deposits and their plate tectonic setting (e.g. Naldrett, 2011). Since cumulus and postcumulus minerals provide information regarding the nature of parental magmas and liquid line of descent, we propose a mineralogical framework to distinguish different types of ultramafic-mafic intrusions in convergent-margin settings.

Modal analyses for ultramafic rocks from two well known Alaskan-type intrusions, Duke Island and Tulameen, and the Giant Mascot intrusion are distinct on the International Union of Geological Sciences (IUGS) classification scheme (Fig. 3). Alaskan-type intrusions lack orthopyroxene and fall exclusively along the olivine-clinopyroxene (Ol-Cpx) join in the hornblende-free plot; hornblende-bearing rocks are predominantly olivine-hornblende clinopyroxenite, hornblende clinopyroxenite, clinopyroxene hornblendite and hornblendite, and minor hornblende wehrlite (Fig. 3b). In contrast, the majority of ultramafic rocks at Giant Mascot, including those hosting Ni-sulphide ores, are hornblende harzburgite, hornblende websterite, two-pyroxene hornblendite, and hornblendite (including plagioclase-bearing pyroxenite), and minor hornblende dunite, olivine-hornblende pyroxenite, and hornblende orthopyroxenite (Fig. 3c). We have used these mineralogical traits to identify orthopyroxene-free Alaskan-type (*sensu stricto*) and orthopyroxene-rich Giant Mascot(GM)-type intrusions that host magmatic Ni-Cu±PGE sulphide mineralization (Table 1). These affiliations rely strongly on petrographic descriptions of the ultramafic rocks. Mineralized gabbroic intrusions in convergent-margin settings that appear to lack an ultramafic component (e.g. Kalatongke, Table 1) or carry unmineralized ultramafic inclusions (e.g. Aguablanca, Table 1) are designated as "gabbroic". In addition, certain ultramafic-mafic suites in the Portneuf-Mauricie Domain, a Proterozoic island arc terrane (Sappin et al., 2009, 2012), that co-crystallized plagioclase and amphibole after orthopyroxene, are provisionally distinguished as a separate orthopyroxene-plagioclase group (Opx-Pl, Table 1).

IMPLICATIONS OF THE MINERALOGICAL CLASSIFICATION

A number of mineralized ultramafic-mafic intrusions that have been documented as Alaskan-type in the literature have a clear GM-type affiliation. These include Gabbro Akarem and Genina Gharbia in Egypt (Helmy and Mogessie, 2001; Helmy and El Mahallawi, 2003; Helmy, 2004) and many intrusions in the Central Asian Orogenic Belt (Xiao et al., 2004, 2010; Table 1). Our reclassification has no impact on paleotectonic interpretations, but may have an important bearing on the interpretation of the petrogenetic history of a given intrusion, and thus critical factors that lead to the formation of an economic magmatic sulphide deposit.

The mineralogical affiliations distinguished above are taken to reflect important petrogenetic variables such as the composition of parental magma, and/or pressure and water fugacity (fH_2O) conditions of crystallization. Previous studies of magmatic Ni-Cu±PGE deposits have shown that parental magma compositions believed to be consistent with the nature and order of crystallization of cumulus phases include (1) moderately magnesian basalt (e.g. ~6–8.5 wt% MgO at Kalatongke: Li et al., 2012); (2) high-MgO basalt (e.g. ~9–13 wt% MgO at Huangshandong: Mao et al., 2014a; Huangshanxi: Mao et al., 2014b; Hongqiling No. 7: Wei et al., 2013; and Erhongwa: Sun et al., 2013b); and (3) for those intrusions particularly enriched in orthopyroxene, a "boninitic" parent has been proposed (e.g. Erbutu: Peng et al., 2013; and the recently documented Xiarihamu intrusion: Li et al., 2015). Due to the presence of hornblende±phlogopite, all authors conclude that parent magmas feeding the intrusions are hydrous, which reduces the stability of plagioclase relative to olivine and pyroxene in the melts. High modal proportions of orthopyroxene may indicate crustal contamination, which potentially has links to early sulphide saturation and ore-forming processes, as explored in the case studies summarized below.

GIANT MASCOT

Studies of the Giant Mascot Ni-Cu-PGE deposit, which is the only significant nickel deposit ever mined in

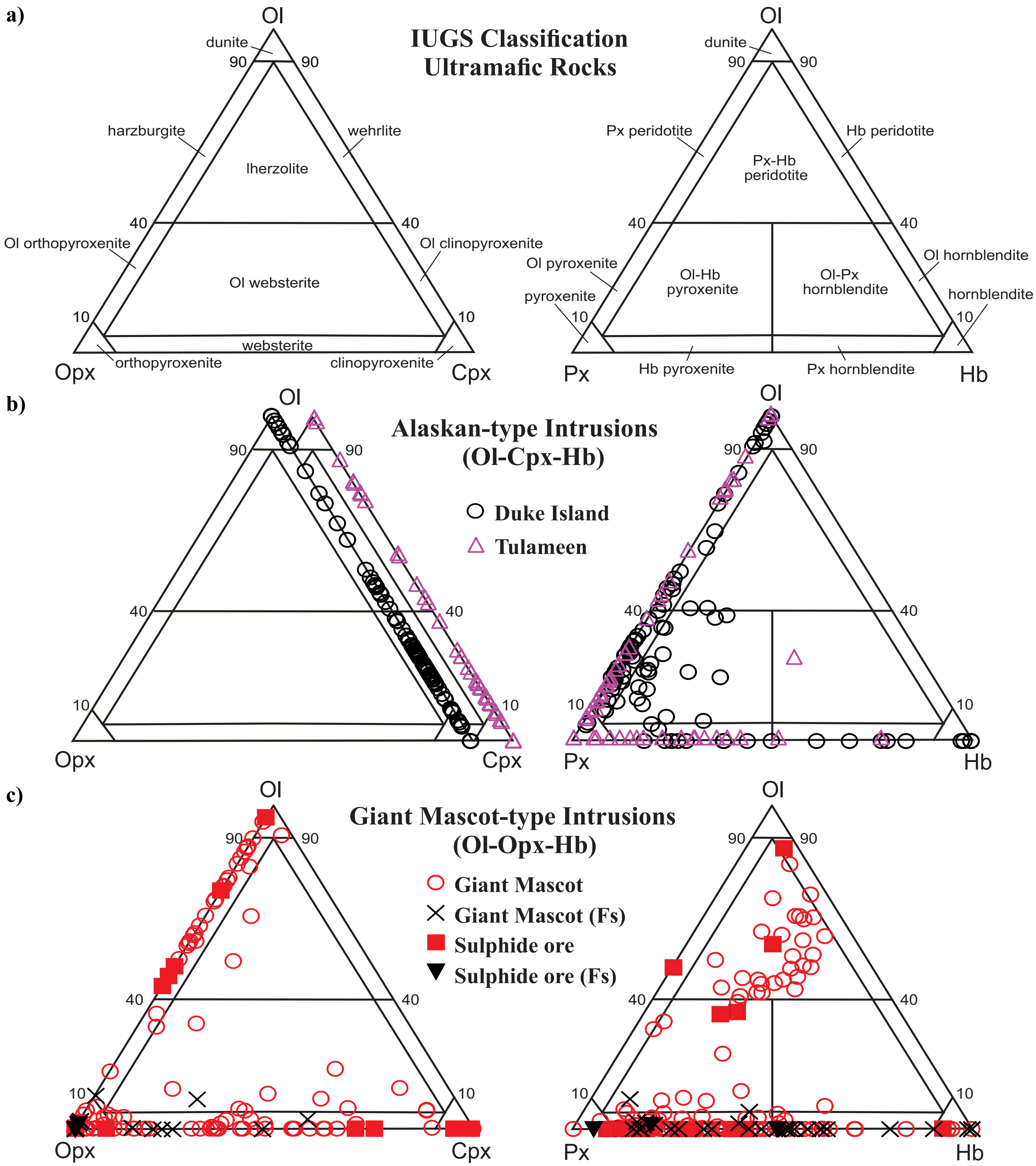

Figure 3. Modal analyses of selected ultramafic-mafic intrusive suites plotted in the IUGS classification scheme: **a)** International Union of Geological Sciences (IUGS) classification of ultramafic rocks (vol%); **b)** Duke Island (Irvine, 1959, Table 7; 1974, Table 18B) and Tulameen (Findlay, 1963, Appendices I and III) Alaskan-type intrusions with characteristic orthopyroxene-absent mineral assemblages; **c)** Giant Mascot ultramafic suite characterized by orthopyroxene-rich, feldspar-free and feldspar(Fs)-bearing (Fs <10%) ultramafic rocks and magmatic Ni-Cu sulphide ores (Muir, 1971, Appendix 1) . Mineral abbreviations: Cpx = clinopyroxene; Hb = hornblende; Ol = olivine; Opx = orthopyroxene; Px = pyroxene.

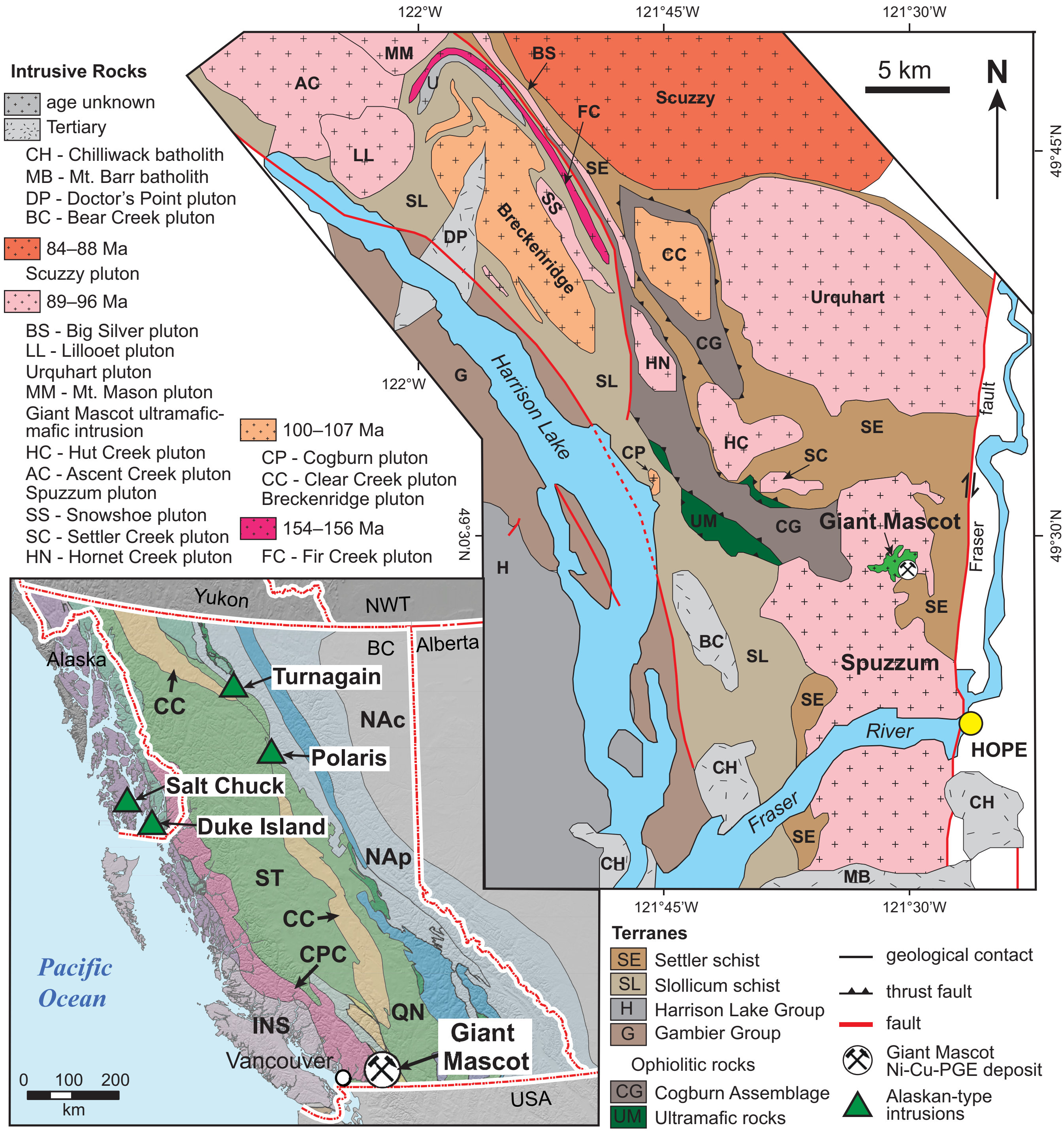

Figure 4. Location of sulphide-rich ultramafic-mafic intrusions in British Columbia and southeastern Alaska (inset) and geology of the Harrison Lake region showing the location of the Giant Mascot ultramafic intrusion and associated Ni-Cu-PGE deposit (after Manor et al., 2015a). Inset shows location of Alaskan-type intrusions referenced in the text and Table 1, and tectonic elements of the northern Cordillera: INS = Insular terranes (Alexander-Wrangellia); arc terranes of Quesnellia (QN) and Stikinia (ST); and Cache-Creek-Bridge River (CC) oceanic terranes; CPC = Coast Plutonic Complex; NAc = North America craton and cover; Nap = North America platform.

British Columbia (1958–1974; Table 1), build upon the pioneering work of Aho (1954, 1956). The deposit is hosted by the Giant Mascot ultramafic intrusion situated at the southeastern margin of the Coast Plutonic Complex (Fig. 4). The ultramafic body forms a small elliptical plug (3 x 1.3 km) intruding amphibolite-facies metasedimentary rocks of the Upper Triassic Settler schist and Late Cretaceous Spuzzum pluton (Fig. 5). A crude zonation of ultramafic lithologies has been mapped ranging from an olivine-rich core (dunite-peri-

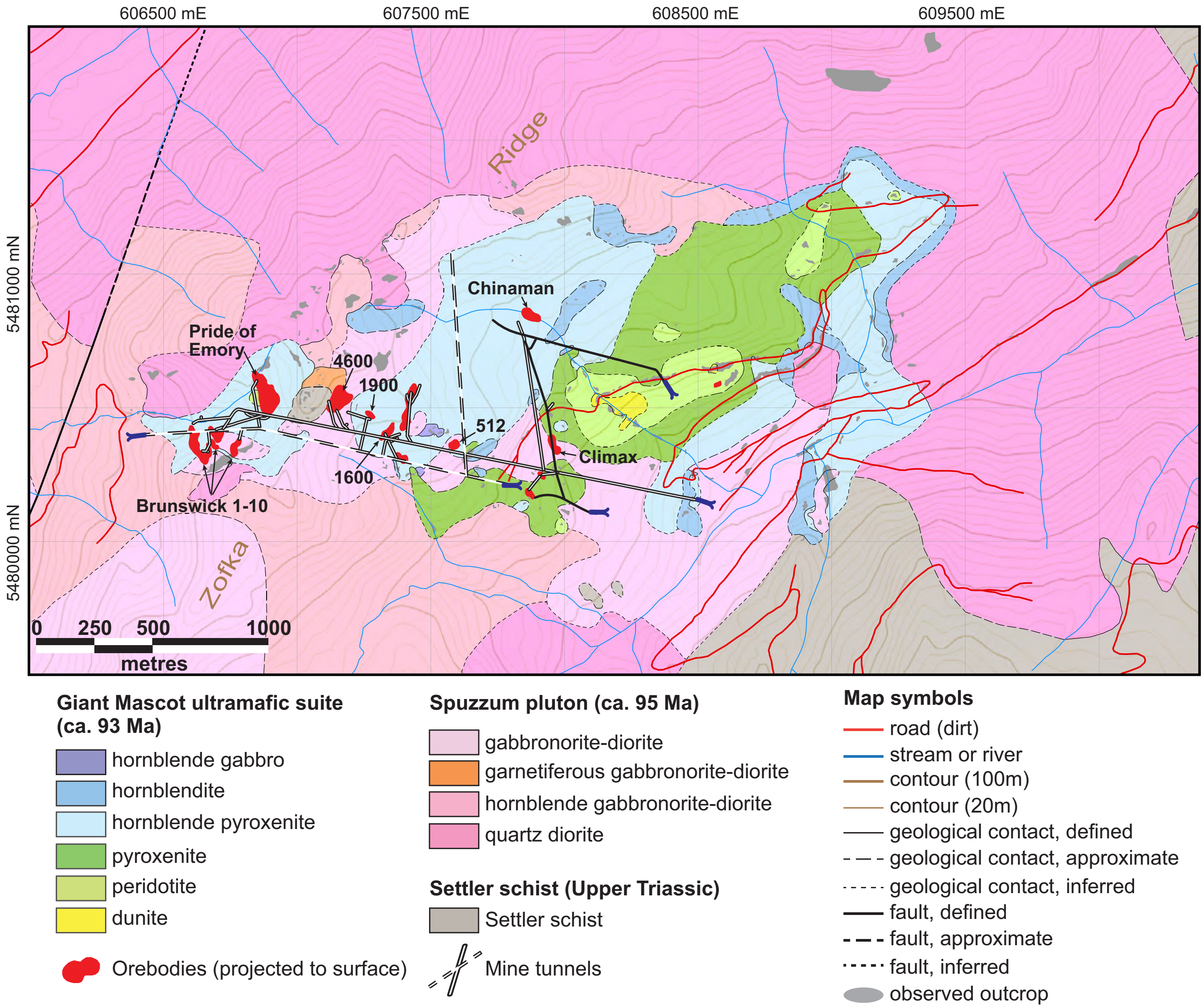

Figure 5. Geology of the Late Cretaceous (ca. 93 Ma) Giant Mascot ultramafic intrusion and surrounding rocks of the Late Cretaceous (ca. 95 Ma) Spuzzum pluton and Upper Triassic Settler schist (after Manor et al., 2015a). Orebodies and mine tunnels shown projected to surface and important orebodies are labeled (projection is NAD83 UTM Zone 10).

dotite) through pyroxenite to a thin, discontinuous rim of hornblendite and hornblende gabbro (Figs. 3, 5; Manor et al., 2014, 2015a). Chemical abrasion-isotope dilution-thermal ionization mass spectrometry (CA-ID-TIMS) U-Pb and $^{40}Ar/^{39}Ar$ geochro-nology on zircon and hornblende/biotite, respectively, has established the Giant Mascot ultramafic suite as Late Cretaceous (ca. 93 Ma) and the Spuzzum diorite as slightly older, but statistically distinct (ca. 95 Ma: Manor, 2014).

Structure of Sulphide Orebodies

The main locus of mineralization at Giant Mascot is oriented at N70°E, passing through Zofka Ridge (Brunswick to Climax orebodies, Fig. 5). The Ni-sulphide ore shoots form steeply plunging, pipe-like and lensoid structures, and atypical, steeply dipping tabular bodies that are ~5–75 m long, ~5–30 m wide and extend ~15–350 m in depth (Manor et al., 2015a). Orebodies are classified as zoned or unzoned, based primarily on textures of the ores (Aho, 1954, 1956). Zoned orebodies are concentrically zoned with disseminated to net-textured sulphides surrounding massive ore, where mineralization is confined to olivine-rich host rocks (dunite and peridotite). Unzoned orebodies are predominantly lensoid to tabular structures containing semimassive to massive mineralization. All orebodies are associated with olivine-bearing ultramafic rocks. We follow the original descriptions of Aho (1954, 1956) and interpret the Giant Mascot orebodies to represent subvertical crustal conduits through which multiple magma pulses ascended. This is evidenced by sharp lithological contacts, reversely zoned ore shoots cored by barren peridotite, and arcuate ore lenses possibly formed by collapse of partially solidified wall-rock cumulates (Manor et al., 2015a).

Ni-Cu-PGE Sulphide Mineralization

Sulphides at Giant Mascot exhibit orthomagmatic textures involving disseminated, net-textured, semimassive, and massive ores, and local Cu-rich veins. The principal base-metal sulphide minerals are pyrrhotite (both monoclinic and hexagonal varieties), pentlandite, chalcopyrite, minor pyrite, and trace amounts of troilite (exsolution flames in pyrrhotite), violarite and polydymite. Sulpharsenide minerals (e.g. gersdorffite, cobaltite, nickeline) are commonly associated with platinum group telluride or bismuthotelluride minerals (e.g. merenskyite, moncheite, palladian melonite), rare arsenide (sperrylite, hollingworthite) and precious metal minerals (hessite, altaite: Manor et al., 2014). The mineralogical and textural relationships between platinum group minerals and sulphide in Giant Mascot ores suggest that PGE were initially collected by an immiscible sulphide liquid and subsequently fractionated and crystallized from a semimetal-rich melt (Manor et al., 2014).

Platinum group elements in the ores are characterized by variable concentrations that define two geographic groupings: iridium-group PGE (IPGE: Ir, Ru) are depleted in the western part of the mineralized zone (WMZ: Pride of Emory and Brunswick cluster; Fig. 5), whereas IPGE are enriched in the central and eastern orebodies (EMZ: all orebodies east of and including 4600; Fig. 5). These differences broadly correlate with the texture and base-metal tenor of sulphide ores (i.e. concentration in 100 wt% sulphide equivalent) such that higher tenor sulphides are more common in disseminated ores of the EMZ, whereas moderate tenor sulphides are more typical of net-textured and massive ores in the WMZ (Manor et al., 2015a). The differences in IPGE concentrations and mantle-normalized enrichment patterns indicate the presence of two distinct parental magmas (Manor et al., in press). Modeling results detailed by Manor et al. (in press) indicate that disseminated ores represent sulphide melt with upgraded metal contents due to extensive interaction and scavenging of metals from silicate melt, whereas net-textured sulphides with low-PGE but high-Cu concentrations, originated from a more fractionated monosulphide solid solution.

Parental Magma and Ore-Forming Mechanisms

Olivine compositions in barren and mineralized ultramafic rocks of the Giant Mascot intrusion range from Fo_{80} to Fo_{89}, with the greatest variation in nickel contents (386–3859 ppm Ni) occuring in mineralized peridotite and pyroxenite (Manor, 2014). Petrographic evidence and modeling results indicate that anomalously high-Ni content in olivine appears to reflect subsolidus equilibration with Ni-rich sulphide liquid, which appeared early in the crystallization history (<20% crystallized) of a moderately magnesian (~9 wt% MgO) parental magma (Manor et al., in press). From the partitioning of Ni and Fe between olivine and sulphide liquid, we determined that the oxygen fugacity of the system at the time of formation of the Giant Mascot ores was relatively reduced (~1 log unit above the quartz-fayalite-magnetite buffer; ΔQFM+1), similar to sulphide deposits formed worldwide in less oxidizing tectonic environments (e.g. rift-related settings). The mechanism for reduction of these parental arc magmas is considered to be assimilation of graphite from the Settler schist. Sulphur isotopic compositions of mineralized samples occupy a narrow range of $\delta^{34}S$ values (-3.4 to -1.3‰) that overlap with those determined for pyrite in graphitic Settler schist ($\delta^{34}S$ = -5.4 to -1.2‰), and are permissive of assimilation of crustal sulphur as a principal mechanism for sulphide saturation (Manor et al., in press). Independent evidence for addition of silica to the parental magma, which also serves to promote sulphide saturation (e.g. Irvine, 1975), is found as abundant xenoliths of diorite and Settler schist, and zircon xenocrysts in Giant Mascot pyroxenite derived from the Spuzzum pluton (Manor et al., 2015a).

TURNAGAIN

The Turnagain Alaskan-type ultramafic-mafic intrusion is hosted in Late Paleozoic metasedimentary and metavolcanic rocks of the Yukon-Tanana terrane in northern British Columbia (Figs. 4, 6). Our study has focused primarily on the youngest hornblende-bearing ultramafic intrusive phase with an anomalous Cu-PGE signature, the DJ/DB zone, and augments previous investigations of the geology and significant Ni-Cu-Co sulphide resource of the Horsetrail zone (Figs. 4, 6; Clark, 1975, 1980; Nixon et al., 1989; Nixon, 1998; Scheel, 2007; Scheel et al., 2009). Below we summarize some aspects of the earlier work in order to place our current studies in context.

Recent fieldwork has confirmed that the elongate (8.5 x 3 km) Turnagain ultramafic body is a composite intrusion with at least four distinct intrusive phases, comprising dunite and wehrlite(±phlogopite), clinopyroxenite(±olivine±hornblende±phlogopite/biotite±magnetite), and minor hornblendite with a dioritic intrusion in the core (Fig. 6). U-Pb Thermal Ionization Mass Spectrometry (TIMS) and $^{40}Ar/^{39}Ar$ geochronology on zircon/titanite and hornblende/phlogopite, respectively, have yielded an Early Jurassic age (ca. 190 Ma) for the intrusion as a whole (Scheel, 2007).

The DJ/DB prospect is hosted by a poorly exposed, younger ultramafic intrusion centred 2.5 km northwest

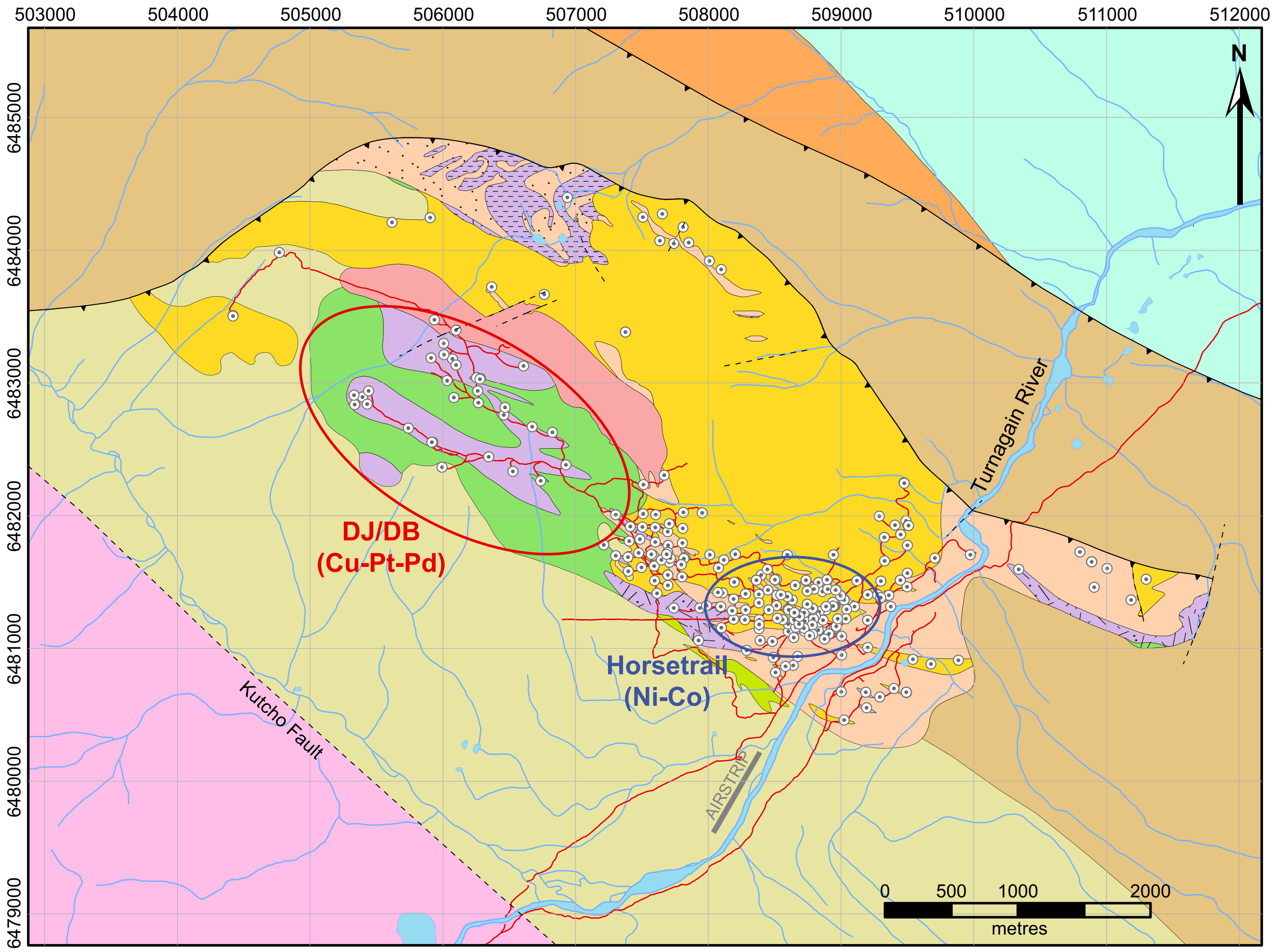

Figure 6. Geology of the Early Jurassic (ca. 190 Ma) Turnagain ultramafic intrusion and host rocks showing the Cu-PGE-enriched DJ/DB zone and the Ni-Co-enriched Horsetrail zone, which is the main Ni-sulphide ore resource (modified from Nixon et al., 2012; projection is NAD83 UTM Zone 9).

of the Horsetrail zone (Fig. 6). The main lithologies are hornblende(±biotite) clinopyroxenite, magnetite-rich (<20 vol%) clinopyroxenite, olivine clinopyroxenite, and hornblendite with minor wehrlite, locally cut by veins of hornblende- or biotite-rich pegmatite, and dioritic dykes of the younger Phase 4 pluton (Fig. 6). The rocks are fine to very coarse grained, interlayered with sharp to gradational (>10 m) contacts, and thicknesses of the different rock types in drill core range from 15 to 155 m (Jackson-Brown et al., 2014).

Ni-Cu-PGE Sulphide Mineralization

The large tonnage, low-grade Ni-sulphide resource defined by Hard Creek Nickel Corporation (Table 1) is hosted by olivine-clinopyroxene cumulates (dunite-wehrlite with minor olivine clinopyroxenite) in the

Horsetrail zone (Fig. 6). Sulphide concentrations (~2–20 vol%) are commonly disseminated with localized net-textures and thin (<20 cm), laterally discontinuous semimassive zones. The principal sulphide minerals are pyrrhotite (~90 vol%), pentlandite with minor chalcopyrite and pyrite, accompanied by trace amounts of violarite, bornite, millerite, molybdenite, valleriite, and mackinawite (Clark, 1975). PGE concentrations in mineralized samples reach ~4 g/t Pt+Pd but are typically much less (<100 ppb) and sulphide-rich samples overall have an average Pt/Pd ratio of ~0.9 and a median ratio of approximately 1 (Hard Creek Nickel Corporation, unpub. data; Scheel, 2007).

The abundance of sulphides in the DJ/DB zone varies greatly (0–55 vol%) and textures range from disseminated and net-textured to locally semimassive. PGE abundances in mineralized samples reach up to 4.9 g/t Pd+Pt with average Pd/Pt ~1 (Jackson-Brown et al., 2014, 2015, in prep). Mineralogical studies of mineralized samples from drill core have been conducted by Jackson-Brown et al. (2014). The principal base-metal sulphides are pyrrhotite and chalcopyrite with minor pyrite and pentlandite, and accessory millerite, sphalerite, bornite, siegenite, marcasite, galena, and molybdenite. Sulpharsenide, sulphantimonide, and arsenide minerals (<1 vol%; <100 µm) include cobaltite, gersdorffite-ullmannite, tucekite, hauchecornite, and nickeline. A variety of platinum group minerals (<40 µm) have been identified (all are platinum and/or palladium species), including sperrylite, sudburyite, palladian melonite, ungavaite, hongshiite, genkinite, and testibiopalladite.

Parental Magma and Ore-Forming Mechanisms

Investigations of the composition of parental magmas and ore-forming processes at Turnagain are currently underway (Jackson-Brown, in prep.). However, some observations from previous work are pertinent here.

The petrology of rocks from the Turnagain Alaskan-type intrusion indicates that it was formed by the successive emplacement and crystallization of primitive, Mg-rich hydrous magma in a subduction setting (Clark, 1975, 1980; Scheel, 2007). Evidence for the primitive nature of the parental magma is found in the most magnesian olivine ($Fo_{92.5}$) in dunite that has not re-equilibrated with chromite. The hydrous nature of the parental magma is supported by (1) primary interstitial phlogopite in olivine-clinopyroxene cumulates; (2) late interstitial to cumulus hornblende in the younger part of the composite intrusion; and (3) late appearance of plagioclase as an interstitial or cumulus phase relative to clinopyroxene and hornblende.

The unusual occurrence of abundant magmatic sulphide in the Turnagain Alaskan-type intrusion is related to the graphitic and sulphidic nature of its wall rocks. Sulphide minerals from the Turnagain intrusion have $\delta^{34}S$ values from +1‰ (i.e. mantle-like) to -9.7‰, shifted towards the composition of pyrite (-17.9‰) from the enclosing graphitic phyllite (Scheel, 2007). These results indicate that crustal sulphur was added to the Turnagain parental magma and presumably aided in achieving sulphide saturation. Inclusions of partially digested, carbonaceous phyllite are abundant in drill core from the Horsetrail zone, and graphite is commonly observed in ultramafic rocks in the mineralized zones. The presence of graphite indicates that, at least locally, the Turnagain parental magma may have had fO_2 near the carbon-carbon monoxide buffer (ΔFMQ = -1) at upper crustal pressures and hydrous conditions. Therefore, the phyllite inclusions acted as both a sulphur source and a reducing agent, allowing the Turnagain intrusion to reach early sulphide saturation in an otherwise oxidizing subduction zone environment.

IMPLICATIONS FOR EXPLORATION

The economic potential of magmatic Ni-Cu-PGE mineralization hosted by a diverse suite of ultramafic-mafic intrusions in convergent-margin tectonic settings is presently underestimated. The prime example of this deposit type in the Canadian Cordillera is the large tonnage, low-grade Ni sulphide endowment of the Turnagain Alaskan-type intrusion, which is currently subeconomic. Other prospects are hosted by Giant Mascot-type intrusions in the southern Coast Plutonic Complex and include the Sable (BC MINFILE 092HNW077), KATT (092GNE044), Jason (092HNW076), and AL (092HNW040), as well as others in the vicinity of the former Giant Mascot mine (and see Pinsent, 2002). Exploration potential in other subduction-related settings is underscored by the recently discovered Xiarihamu Ni-sulphide deposit in the East Kunlun orogenic belt at the northern margin of the Tibetan Plateau, western China. Despite its current subeconomic status, this magmatic Ni-Cu sulphide deposit contains 100 Mt of ore at an average grade of 0.8 wt% Ni and 0.1 wt% Cu, which makes it one of the 20 largest magmatic Ni deposits in the world (Li et al., 2015). Like most of the other deposits in convergent-margin settings in China, ultramafic host rocks have Giant Mascot-type affinity (Table 1).

Factors that appear fundamental to the genesis of potentially economic magmatic Ni-Cu±PGE deposits in subduction-related settings are similar to those that determine world-class Ni deposits in other tectonic environments. These include (1) primitive MgO- and Ni-rich parental magmas; (2) favourable wall rocks that can contribute crustal sulphur and/or reductants to relatively oxidized and hydrous arc magmas, thereby promoting early sulphide saturation and formation of an immiscible sulphide melt; and (3) restrictive conduit systems capable of channelling new influxes of metal-laden parent magma and serving as suitable traps for the collection of upgraded Ni-Cu-PGE-enriched sulphides.

ACKNOWLEDGEMENTS

Funding for this collaborative project is provided by Natural Resources Canada through the Geological Survey of Canada's Targeted Geoscience Initiative 4 (TGI-4) Nickel-Copper-PGE-Chrome Ore System Project, and the British Columbia Geological Survey. Additional funding was provided by Society of Economic Geologists, Canadian Foundation Graduate Student Research Grants awarded to Matthew Manor and Sarah Jackson-Brown in 2013, and an NSERC Discovery Grant to James Scoates. We thank Mark Jarvis and Tony Hitchins of Hard Creek Nickel Corporation for logistical support, and access to drill core and proprietary data. The manuscript benefited from a thorough review by Dr. Alex Zagorevski and editorial comments by Dr. Lawrence Aspler.

REFERENCES

Aho, A.E., 1954. Geology and ore deposits of the property of Pacific Nickel Mines near Hope, British Columbia; Ph.D. thesis, University of California, California, 148 p.

Aho, A.E., 1956. Geology and genesis of ultrabasic nickel-copper-pyrrhotite deposits at the Pacific Nickel Property, southwestern British Columbia; Economic Geology, v. 51, p. 441–481.

Ames, D.E. and Houlé, M.G., 2011. Overview of the Targeted Geoscience Initiative 4 Nickel-Copper-Platinum Group Elements-Chromium Project (2010–2015) — Mafic to Ultramafic Ore Systems: Footprint, Fertility and Vectors, *In:* Summary of Field Work and Other Activities 2011; Ontario Geological Survey, Open File Report 6270, p. 37-1 to 37-7.

Ames D.E., Dare S.A., Hanley, J.J. Hollings, P., Jackson, S., Jugo, P.J., Kontak, D., Linnen R., and Samson, I.M., 2012. Update on Research Activities in the Targeted Geoscience Initiative 4 Magmatic-Hydrothermal Nickel-Copper-Platinum Group Elements Ore System subproject: System Fertility and Ore Vectors, *In:* Summary of Field Work and Other Activities 2012; Ontario Geological Survey, Open File Report 6280, p. 41-1 to 41-11.

Branquet, Y., Gumiaux, C., Sizaret, S., Barbanson, L., Wang, B., Cluzel, D., Li, G., and Delaunay, A., 2012. Synkinematic mafic/ultramafic sheeted intrusions: emplacement mechanism and strain restoration of the Permian Huangshan Ni–Cu ore belt (Eastern Tianshan, NW China); Journal of Asian Earth Sciences, v. 56, p. 240–257. doi:10.1016/j.jseaes.2012.05.021.

Casquet, C., Galindo, C., Tornos, F., Velasco, F., and Canales, A., 2001. The Aguablanca Cu-Ni ore deposit (Extremadura, Spain), a case of synorogenic orthomagmatic mineralization: age and isotope composition of magmas (Sr, Nd) and ore (S); Ore Geology Reviews, v. 18, p. 237–250.

Clark, T., 1975. Geology of an ultramafic complex on the Turnagain River, northwestern British Columbia; Ph.D. thesis, Queen's University, Kingston, Ontario, 453 p.

Clark, T., 1980. Petrology of the Turnagain ultramafic complex, northwestern British Columbia; Canadian Journal of Earth Sciences, v. 17, p. 744–757. doi:10.1139/e80-071

Findlay, D.C., 1963. Petrology of the Tulameen ultramafic complex, Yale District, British Columbia; Ph.D. thesis, Queen's University, Kingston, Ontario, 415 p.

Gao, J.-F., Zhou, M.-F., Lightfoot, P.C., Wang, C.Y., and Qi, L., 2012. Origin of PGE-poor and Cu-rich magmatic sulfides from the Kalatongke deposit, Xinjiang, Northwest China; Economic Geology, v. 107, p. 481–506.

Gao, J.-F., Zhou, M.-F., Lightfoot, P.C., Wang, C.Y., Qi, L., and Sun, M., 2013. Sulfide saturation and magma emplacement in the formation of the Permian Huangshandong Ni-Cu sulfide deposit, Xinjiang, northwestern China; Economic Geology, v. 108, p. 1833–1848. doi:10.2113/econgeo.108.8.1833

Guillot, S., Hattori, K., Agard, P., Schwartz, S., and Vidal, O., 2009. Exhumation processes in oceanic and continental subduction contexts: a review, *In:* Subduction Zone Geodynamics, (ed.) S. Lallemand and F. Funiciello, F.; Springer, Berlin Heidelberg, p. 175–205.

Han, B., Ji, J., Song, B., Chen, L., and Li, Z., 2004. SHRIMP zircon U-Pb ages of Kalatongke No. 1 and Huangshandong Cu-Ni-bearing mafic-ultramafic complexes, North Xinjiang, and geological implications; Chinese Science Bulletin, v. 49, p. 2424–2429. doi:10.1007/BF03183432

Han, C., Xiao, W., Zhao, G., Su, B.-X., Sakyi, P.A., Ao, S., Wan, B., Zhang, J., and Zhang, Z., 2013. SIMS U-Pb zircon dating and Re-Os isotopic analysis of the Hulu Cu-Ni deposit, eastern Tianshan, Central Asian Orogenic Belt, and its geological significance; Journal of Geosciences, v. 58, p. 251–270. doi:10.3190/jgeosci.146

Helmy, H.M., 2004. Cu–Ni–PGE mineralization in the Genina Gharbia mafic–ultramafic intrusion, Eastern Desert, Egypt; The Canadian Mineralogist, v. 42, p. 351–370. doi:10.2113/gscanmin.42.2.351

Helmy, H.M. and Mogessie, A., 2001. Gabbro Akarem, Eastern Desert, Egypt: Cu–Ni–PGE mineralization in a concentrically zoned mafic–ultramafic complex; Mineralium Deposita, v. 36, p. 58–71.

Helmy, H.M. and El Mahallawi, M.M., 2003. Gabbro Akarem mafic-ultramafic complex, Eastern Desert, Egypt: a Late Precambrian analogue of Alaskan-type complexes; Mineralogy and Petrology, v. 77, p. 85–108. doi:10.1007/s00710-001-0185-9

Helmy, H.M., Ahmed, A.H., Kagami, A., and Arai, S., 2005. Sm/Nd and platinum-group element geochemistry of a late-Precambrian Alaskan-type complex from the Eastern Desert of Egypt, *In:* Proceedings; 10th International Platinum Symposium, Oulu, Finland, 2005, p. 101–104.

Helmy, H.M., Abd El-Rahman, Y.M., Yoshikawa, M., Shibata, T., Arai, S., Tamura, A., and Kagami, H., 2014. Petrology and Sm–Nd dating of the Genina Gharbia Alaskan-type complex (Egypt): Insights into deep levels of Neoproterozoic island arcs; Lithos, v. 198–199, p. 263–280. doi:10.1016/j.lithos.2014.03.028

Himmelberg, G.R. and Loney, R.A., 1995. Characteristics and petrogenesis of Alaskan-type ultramafic-mafic intrusions, southeastern Alaska; United States Geological Survey, Professional Paper 1564, 47 p.

Holt, S.P., Shepard, J.G., Thorne, R.L., Tolonen, A.W., and Fosse, E.L., 1948. Investigation of the Salt Chuck copper mine, Kasaan Peninsula, Prince of Wales Island, southeastern Alaska; United States Bureau of Mines, Report of Investigations 4358, 16 p.

Irvine, T.N., 1959. The ultramafic complex and related rocks of Duke Island, southeastern Alaska; Ph.D. thesis, California Institute of Technology, Pasadena, California, 320 p.

Irvine, T.N., 1974. Petrology of the Duke Island ultramafic complex, southeastern Alaska; Geological Society of America Memoirs, v. 138, 240 p.

Irvine, T.N., 1975. Crystallization sequences in the Muscox intrusion and other layered intrusions – II. Origin of chromitite layers and similar deposits of other magmatic ores; Geochimica et Cosmochimica Acta, v. 39, p. 991–1020.

Jackson-Brown, S., in prep. Origin of the Cu-PGE-rich sulphide mineralization in the DJ/DB zone of the Turnagain Alaskan-type intrusion, British Columbia; M.Sc. thesis, University of British Columbia, Vancouver, British Columbia.

Jackson-Brown, S., Scoates, J.S., Nixon, G.T., and Ames, D.E., 2014. Mineralogy of sulphide, arsenide, and platinum group minerals from the DJ/DB Zone of the Turnagain Alaskan-type ultramafic intrusion, north-central British Columbia, *In:* Geological Fieldwork 2013; British Columbia Ministry of Energy and Mines, British Columbia Geological Survey, Paper 2014-1, p. 157–168.

Jackson-Brown, S., Scoates, J.S., Nixon, G.T., and Ames, D.E., 2015, Preliminary observations of the geology, mineralogy and geochemistry of the DJ/DB zone of the Turnagain intrusion, north-central British Columbia; Geological Survey of Canada, Open File 7871.

Johan, Z., 2002. Alaskan-type complexes and their platinum-group-element mineralization, *In:* The Geology, Geochemistry, Mineralogy and Mineral Beneficiation of Platinum-Group Elements, (ed.) L.J. Cabri; Canadian Institute of Mining, Metallurgy and Petroleum, Special Volume 54, p. 669–719.

Li, C., Zhang, M., Fu, P., Qian, Z., Hu, P., and Ripley, E.M., 2012. The Kalatongke magmatic Ni–Cu deposits in the Central Asian Orogenic Belt, NW China: product of slab window magmatism?; Mineralium Deposita, v. 47, p. 51–67. doi:10.1007/s00126-011-0354-7

Li, C., Zhang, Z., Li, W., Wang, Y., Sun, T., and Ripley, E.M., 2015. Geochronology, petrology and Hf–S isotope geochemistry of the newly-discovered Xiarihamu magmatic Ni–Cu sulfide deposit in the Qinghai–Tibet plateau, western China; Lithos, v. 216-217, p. 224–240. doi:10.1016/j.lithos.2015.01.003

Loney, R.A. and Himmelberg, G.R., 1992. Petrogenesis of the Pd-rich intrusion at Salt Chuck, Prince of Wales Island; an early Paleozoic Alaskan-type ultramafic body; The Canadian Mineralogist, v. 30, p. 1005–1022.

Lü, L., Mao, J., Li, H., Pirajno, F., Zhang, Z., and Zhou, Z., 2011. Pyrrhotite Re–Os and SHRIMP zircon U–Pb dating of the Hongqiling Ni–Cu sulfide deposits in northeast China; Ore Geology Reviews, v. 43, p. 106–119. doi:10.1016/j.oregeorev.2011.02.003.

MacTavish, A.D., 1999. The mafic-ultramafic intrusions of the Atikokan-Quetico area, northwestern Ontario; Ontario Geological Survey, Open File Report 5997, 127 p.

Manor, M.J., 2014. Convergent margin Ni-Cu-PGE deposits: geology, geochronology, and geochemistry of the Giant Mascot magmatic sulphide deposit, Hope, British Columbia; M.Sc. thesis, University of British Columbia, Vancouver, British Columbia, 371 p.

Manor, M.J., Scoates, J.S., Nixon, G.T., and Ames, D.E., 2014. Platinum-group mineralogy of the Giant Mascot Ni-Cu-PGE deposit, Hope, BC, *In:* Geological Fieldwork 2013; British Columbia Ministry of Energy and Mines, British Columbia Geological Survey, Paper 2014-1, p. 141–156.

Manor, M.J., Wall, C.J., Nixon, G.T., Scoates, J.S., Pinsent, R.H., and Ames, D.E., 2014. Preliminary geology and geochemistry of the Giant Mascot ultramafic-mafic intrusion, Hope, southwestern British Columbia; Geological Survey of Canada Open File 7570, scale: 1:10 000 (also British Columbia Ministry of Energy and Mines, British Columbia Geological Survey, Open File 2014-03).

Manor, M.J., Wall, C.J., Friedman, R.M., Gabites, J., Nixon, G.T., Scoates, J.S., and Ames, D.E., 2015. Geology, geochronology and Ni-Cu-PGE orebodies of the Giant Mascot ultramafic intrusion, Hope, southwestern British Columbia; British Columbia Ministry of Energy and Mines, British Columbia Geological Survey, Geoscience Map 2015-01, scale: 1:10 000 (2 sheets).

Manor, M.J., Scoates, J.S., Nixon, G.T., and Ames, D.E., in press. The Giant Mascot Ni-Cu-PGE deposit, southwestern British Columbia: mineralized conduits and sulphide saturation mechanisms in a convergent margin tectonic setting: Economic Geology.

Mao, J.W., Pirajno, F., Zhang, Z.H., Chai, F.M., Wu, H., Chen, S.P., Cheng, L.S., Yang, J.M., and Zhang, C.Q., 2008. A review of the Cu–Ni sulphide deposits in the Chinese Tianshan and Altay orogens (Xinjiang Autonomous Region, NW China): Principal characteristics and ore-forming processes; Journal of Asian Earth Sciences, Geodynamics and Metallogeny of the Altaid Orogen, v. 32, p. 184–203. doi:10.1016/j.jseaes.2007.10.006

Mao, Y.-J., Qin, K.-Z., Li, C., and Tang, D.-M., 2014a. A modified genetic model for the Huangshandong magmatic sulfide deposit in the Central Asian Orogenic Belt, Xinjiang, western China; Mineralium Deposita, v. 50, p. 65–82. doi:10.1007/s00126-014-0524-5.

Mao, Y.-J., Qin, K.-Z., Li, C., Xue, S.-C., and Ripley, E.M., 2014b. Petrogenesis and ore genesis of the Permian Huangshanxi sulfide ore-bearing mafic-ultramafic intrusion in the Central Asian Orogenic Belt, western China; Lithos, v. 200–201, p. 111–125. doi:10.1016/j.lithos.2014.04.008

Mota-e-Silva, J., Ferreira Filho, C.F., Bühn, B., and Dantas, E.L., 2011. Geology, petrology and geochemistry of the "Americano do Brasil" layered intrusion, central Brazil, and its Ni–Cu sulfide deposits; Mineralium Deposita, v. 46, p. 57–90. doi:10.1007/s00126-010-0312-9.

Mowat, U.G., 2013. Sampling of the Star 5, 6, 7, 10 and 12 claims; British Columbia Assessment Report 34297, 111 p.

Mudd, G.M. and Jowitt, S.M., 2014. A detailed assessment of global nickel resource trends and endowments; Economic Geology, v. 109, p. 1813–1841.

Muir, J.E., 1971. A study of the petrology and ore genesis of the Giant Nickel 4600 orebody, Hope, B.C.; M.Sc. thesis, University of Toronto, Toronto, Ontario, 134 p.

Naldrett, A.J., 2010. Secular variation of magmatic sulfide deposits and their source magmas; Economic Geology, v. 105, p. 669–688.

Naldrett, A.J., 2011. Fundamentals of magmatic sulfide deposits; Reviews in Economic Geology, v. 17, p. 1–50.

Nilson, A.A., 1981. The nature of the Americano do Brasil mafic-ultramafic complex and associated sulfide mineralization, Goias, Brazil; Ph.D. thesis, University of Western Ontario, London, Ontario, 488 p.

Nixon, G.T., 1998. Ni-Cu sulfide mineralization in the Turnagain Alaskan-type complex; a unique magmatic environment, *In:* Geological Fieldwork 1997; Ministry of Employment and Investment, British Columbia Geological, Survey Paper 1998-1, p. 18.1–18.11.

Nixon, G.T., Ash, C.A., Connelly, J.N., and Case, G., 1989. Geology and noble metal geochemistry of the Turnagain ultramafic complex, northern British Columbia; British Columbia Ministry of Energy, Mines and Petroleum Resources, British Columbia Geological Survey, Open File 1989-18, scale: 1:16 000.

Nixon, G.T., Cabri, L.J., and Laflamme, J.H.G., 1990. Platinum-group-element mineralization in lode and placer deposits associated with the Tulameen Alaskan-type complex, British-Columbia; The Canadian Mineralogist, v. 28, p. 503–535.

Nixon, G.T., Hammack, J.L., Ash, C.A., Cabri, L.J., Case, G., Connelly, J.N., Heaman, L.M., Laflamme, J.H.G., Nuttall, C., Paterson, W.P.E., and Wong, R.H., 1997. Geology and platinum-group-element mineralization of Alaskan-type ultramafic-mafic complexes in British Columbia; Ministry of Employment and Investment, British Columbia Geological Survey, Bulletin 93, 141 p.

Nixon, G.T., Hitchins, A.C., and Ross, G.P., 2012. Geology of the Turnagain ultramafic intrusion, northern British Columbia; British Columbia Ministry of Energy and Mines, British Columbia Geological Survey, Open File 2012-05, scale: 1: 10 000.

Noble, J.A. and Taylor, H.P., Jr., 1960. Correlation of the ultramafic complexes of southeastern Alaska with those of other parts of North America and the world; Report of the International Geological Congress, Part 13, p. 188–197.

Parker, J.R., 1998. Geology of nickel-copper-chromite deposits and cobalt-copper deposits at Werner-Rex-Bug lakes, English River Subprovince, northwestern Ontario; Ontario Geological Survey, Open File Report 5975, 178 p.

Peng, R., Zhai, Y., Li, C., and Ripley, E.M., 2013. The Erbutu Ni-Cu deposit in the Central Asian Orogenic Belt: a Permian magmatic sulfide deposit related to boninitic magmatism in an arc setting; Economic Geology, v. 108, p. 1879–1888. doi:10.2113/econgeo.108.8.1879.

Pettigrew, N.T. and Hattori, K.H., 2006. The Quetico intrusions of Western Superior Province: Neo-Archean examples of Alaskan/Ural-type mafic–ultramafic intrusions; Precambrian Research, v. 149, p. 21–42. doi:10.1016/j.precamres.2006.06.004

Pettigrew, N.T., Hattori, K.H., and Percival, J.A., 2000. Samuels Lake intrusion: a Late Archean Cu-Ni-PGE-bearing mafic-ultramafic complex in the western Quetico Subprovince, northwestern Ontario; Geological Survey of Canada, Current Research 2000-C20, 8 p.

Piña, R., Lunar, R., Ortega, L., Gervilla, F., Alapieti, T., and Martínez, C., 2006. Petrology and geochemistry of mafic-ultramafic fragments from the Aguablanca Ni-Cu ore breccia, southwest Spain; Economic Geology, v. 101, p. 865–881.

Piña, R., Gervilla, F., Ortega, L., and Lunar, R., 2008. Mineralogy and geochemistry of platinum-group elements in the Aguablanca Ni-Cu deposit (SW Spain); Mineralogy and Petrology, v. 92, p. 259–282.

Piña, R., Romeo, I., Ortega, L., Lunar, R., Capote, R., Gervilla, F., Tejero, R., and Quesada, C., 2010. Origin and emplacement of the Aguablanca magmatic Ni-Cu-(PGE) sulfide deposit, SW Iberia: A multidisciplinary approach; Geological Society of America Bulletin, v. 122, p. 915–925. doi:10.1130/B30046.1

Piña, R., Gervilla, F., Ortega, L., and Lunar, R., 2012. Geochemical constraints on the origin of the Ni–Cu sulfide ores in the Tejadillas prospect (Cortegana Igneous Complex, SW Spain); Resource Geology, v. 62, p. 263–280. doi:10.1111/j.1751-3928.2012.00194.x

Pinsent, R.H., 2002. Ni-Cu-PGE potential of the Giant Mascot and Cogburn ultramafic-mafic bodies, Harrison-Hope area, southwestern British Columbia (092H), *In:* Geological Fieldwork 2001; British Columbia Ministry of Energy and Mines, British Columbia Geological Survey, Paper 2002-1, p. 211–236.

Qin, K., Su, B., Sakyi, P.A., Tang, D., Li, X., Sun, H., Xiao, Q., and Liu, P., 2011. SIMS zircon U-Pb geochronology and Sr-Nd isotopes of Ni-Cu-bearing mafic-ultramafic intrusions in Eastern Tianshan and Beishan in correlation with flood basalts in Tarim Basin (NW China): Constraints on a ca. 280 Ma mantle plume; American Journal of Science, v. 311, p. 237–260. doi:10.2475/03.2011.03

Ripley, E.M., Li, C., and Thakurta, J., 2005. Magmatic Cu-Ni-PGE mineralization at a convergent plate boundary: Preliminary mineralogic and isotopic studies of the Duke Island Complex, Alaska, *In:* Mineral Deposit Research, (ed.) P.D.J. Mao, and D.F.P. Bierlein; Meeting the Global Challenge, Springer Berlin Heidelberg, p. 49–51.

Romeo, I., Lunar, R., Capote, R., Quesada, C., Dunning, G.R., Pina, R., and Ortega, L., 2006. U-Pb age constraints on Variscan magmatism and Ni-Cu-PGE metallogeny in the Ossa-Morena Zone (SW Iberia); Journal of the Geological Society of London, v. 163, p. 837–846. doi:10.1144/0016-76492005-065

Saleeby, J.B., 1992. Age and tectonic setting of the Duke Island ultramafic intrusion, southeast Alaska; Canadian Journal of Earth Sciences, v. 29, p. 506–522.

Sappin, A.-A., Constantin, M., Clark, T., and van Breemen, O., 2009. Geochemistry, geochronology, and geodynamic setting of Ni–Cu±PGE mineral prospects hosted by mafic and ultramafic intrusions in the Portneuf–Mauricie Domain, Grenville Province, Quebec; Canadian Journal of Earth Sciences, v. 46, p. 331–353. doi:10.1139/E09-022

Sappin, A.-A., Constantin, M., and Clark, T., 2011. Origin of magmatic sulfides in a Proterozoic island arc—an example from the Portneuf–Mauricie Domain, Grenville Province, Canada; Mineralium Deposita, v. 46, p. 211–237. doi:10.1007/s00126-010-0321-8

Sappin, A.-A., Constantin, M., and Clark, T., 2012. Petrology of mafic and ultramafic intrusions from the Portneuf–Mauricie Domain, Grenville Province, Canada: Implications for plutonic complexes in a Proterozoic island arc; Lithos, v. 154, p. 277–295. doi:10.1016/j.lithos.2012.07.016

Scheel, J.E., 2007. Age and origin of the Turnagain Alaskan-type intrusion and associated Ni-sulphide mineralization, north-central British Columbia, Canada; M.Sc. thesis, The University of British Columbia, Vancouver, British Columbia, 210 p.

Scheel, J.E., Scoates, J.S., and Nixon, G.T., 2009. Chromian spinel in the Turnagain Alaskan-type ultramafic intrusion, northern British Columbia, Canada; The Canadian Mineralogist, v. 47, p. 63–80. doi:10.3749/canmin.47.1.63

Scoates, R.F.J., 1972. Ultramafic rocks and associated copper-nickel sulphide ores, Gordon Lake, Ontario; Ph.D. thesis, University of Manitoba, Winnipeg, Manitoba, 206 p.

Simard, R.-L., Dostal, J., and Roots, C.F., 2003. Development of late Paleozoic volcanic arcs in the Canadian Cordillera: an example from the Klinkit Group, northern British Columbia and southern Yukon; Canadian Journal of Earth Sciences, v. 40, p. 907–924. doi:10.1139/e03-025

Su, B.-X., Qin, K.-Z., Santosh, M., Sun, H., and Tang, D.-M., 2013. The Early Permian mafic–ultramafic complexes in the Beishan Terrane, NW China: Alaskan-type intrusives or rift cumulates?; Journal of Asian Earth Sciences, v. 66, p. 175–187. doi:10.1016/j.jseaes.2012.12.039

Sun, T., Qian, Z.-Z., Deng, Y.-F., Li, C., Song, X.-Y., and Tang, Q., 2013a. PGE and isotope (Hf-Sr-Nd-Pb) constraints on the origin of the Huangshandong magmatic Ni-Cu sulfide deposit in the Central Asian Orogenic Belt, northwestern China; Economic Geology, v. 108, p. 1849–1864. doi:10.2113/econgeo.108.8.1849

Sun, T., Qian, Z.-Z., Li, C., Xia, M.-Z., and Yang, S.-H., 2013b. Petrogenesis and economic potential of the Erhongwa mafic–ultramafic intrusion in the Central Asian Orogenic Belt, NW China: Constraints from olivine chemistry, U–Pb age and Hf isotopes of zircons, and whole-rock Sr–Nd–Pb isotopes; Lithos, v. 182–183, p. 185–199. doi:10.1016/j.lithos.2013.10.004

Taylor, H.P., Jr., and Noble, J.A., 1960. Origin of the ultramafic complexes in southeastern Alaska; Report of the International Geological Congress, Part 13, p. 175–187.

Taylor, H.P., Jr., 1967. The zoned ultramafic complexes of southeastern Alaska, *In:* Ultramafic and Related Rocks, (ed.) P.J. Wyllie; Wiley and Sons, New York, p. 97–121.

Tornos, F., Casquet, C., Galindo, C., Velasco, F., and Canales, A., 2001. A new style of Ni-Cu mineralization related to magmatic breccia pipes in a transpressional magmatic arc, Aguablanca, Spain; Mineralium Deposita, v. 36, p. 700–706.

Tornos, F., Galindo, C., Casquet, C., Rodríguez Pevida, L., Martínez, C., Martínez, E., Velasco, F., and Iriondo, A., 2006. The Aguablanca Ni–(Cu) sulfide deposit, SW Spain: geologic and geochemical controls and the relationship with a midcrustal layered mafic complex; Mineralium Deposita, v. 41, p. 737–769.

Wei, B., Wang, C.Y., Li, C., and Sun, Y., 2013. Origin of PGE-depleted Ni-Cu sulfide mineralization in the Triassic Hongqiling No. 7 orthopyroxenite intrusion, Central Asian Orogenic Belt, northeastern China; Economic Geology, v. 108, p. 1813–1831. doi:10.2113/econgeo.108.8.1813

Weiser, T.W., 2002. Platinum-group minerals (PGM) in placer deposits, *In:* The geology, geochemistry, mineralogy and mineral beneficiation of platinum-group elements, (ed.) L.J. Cabri; Canadian Institute of Mining, Metallurgy and Petroleum, Special Volume 54, p. 721–756.

Wu, F., Wilde, S.A., Zhang, G., and Sun, D., 2004. Geochronology and petrogenesis of the post-orogenic Cu–Ni sulfide-bearing mafic–ultramafic complexes in Jilin Province, NE China; Journal of Asian Earth Sciences, Phanerozoic Continental Growth in Central Asia, v. 23, p. 781–797. doi:10.1016/S1367-9120(03)00114-7

Xia, M.-Z., Jiang, C.-Y., Li, C., and Xia, Z.-D., 2013. Characteristics of a newly discovered Ni-Cu sulfide deposit hosted in the Poyi ultramafic intrusion, Tarim Craton, NW China; Economic Geology, v. 108, p. 1865–1878. doi:10.2113/econgeo.108.8.1865

Xiao, W.-J., Zhang, L.-C., Qin, K.-Z., Sun, S., and Li, J.-L., 2004. Paleozoic accretionary and collisional tectonics of the eastern Tianshan (China): Implications for the continental growth of central Asia; American Journal of Science, v. 304, p. 370–395. doi:10.2475/ajs.304.4.370

Xiao, W.J., Mao, Q.G., Windley, B.F., Han, C.M., Qu, J.F., Zhang, J.E., Ao, S.J., Guo, Q.Q., Cleven, N.R., Lin, S.F., Shan, Y.H., and Li, J.L., 2010. Paleozoic multiple accretionary and collisional processes of the Beishan orogenic collage; American Journal of Science, v. 310, p. 1553–1594. doi:10.2475/10.2010.12

Xie, W., Song, X.-Y., Deng, Y.-F., Wang, Y.-S., Ba, D.-H., Zheng, W.-Q., and Li, X.-B., 2012. Geochemistry and petrogenetic implications of a Late Devonian mafic–ultramafic intrusion at the southern margin of the Central Asian Orogenic Belt; Lithos, v. 144–145, p. 209–230. doi:10.1016/j.lithos.2012.03.010

Xie, W., Song, X.-Y., Chen, L.-M., Deng, Y.-F., Zheng, W.-Q., Wang, Y.-S., Ba, D.-H., Yin, M.-H., and Luan, Y., 2014. Geochemistry insights on the genesis of the subduction-related Heishan magmatic Ni-Cu-(PGE) deposit, Gansu, northwestern China, at the southern margin of the Central Asian Orogenic Belt; Economic Geology, v. 109, p. 1563–1583. doi:10.2113/econgeo.109.6.1563

Zhang, Z., Mao, J., Chai, F., Yan, S., Chen, B., and Pirajno, F., 2009. Geochemistry of the Permian Kalatongke mafic intrusions, northern Xinjiang, northwest China: Implications for the genesis of magmatic Ni-Cu sulfide deposits; Economic Geology, v. 104, p. 185–203. doi:0.2113/gsecongeo.104.2.185

Zhang, C.-L., Li, Z.-X., Li, X.-H., Xu, Y.-G., Zhou, G., and Ye, H.-M., 2010. A Permian large igneous province in Tarim and Central Asian orogenic belt, NW China: Results of a ca. 275 Ma mantle plume?; Geological Society of America Bulletin, v. 122, p. 2020–2040. doi:10.1130/B30007.1

Zhang, M., Li, C., Fu, P., Hu, P., and Ripley, E.M., 2011. The Permian Huangshanxi Cu–Ni deposit in western China: intrusive–extrusive association, ore genesis, and exploration implications; Mineralium Deposita, v. 46, p. 153–170. doi:10.1007/s00126-010-0318-3